Energy transfer versus charge separation in hybrid systems of semiconductor quantum dots and Ru-dyes as potential co-sensitizers of TiO_2-based solar cells

Sixto Giménez,[1,a)] Andrey L. Rogach,[2,a)] Andrey A. Lutich,[3] Dieter Gross,[3] Andreas Poeschl,[3] Andrei S. Susha,[2] Ivan Mora-Seró,[1] Teresa Lana-Villarreal,[4] and Juan Bisquert[1]

[1]*Grup de dispositius Fotovoltaics i Optoelectrònics, Departament de Física, Universitat Jaume I, 12071 Castelló, Spain*
[2]*Department of Physics and Materials Science and Centre for Functional Photonics (CFP), City Universtiy of Hong Kong, Tat Chee Avenue, Hong Kong*
[3]*Photonics and Optoelectronics Group, Physics Department and Center for Nanoscience (CeNS), Ludwig-Maximilians-Universität München, Amalienstr. 54, D-80799 Munich, Germany*
[4]*Departament de Química-Física i Institut Universitari d'Electroquímica, Universitat d'Alacant, Ap. 99, E-03080 Alacant, Spain*

(Received 13 April 2011; accepted 6 June 2011; published online 14 July 2011)

Hybrid structures of colloidal quantum dots (QDs) with Ru-dyes have been studied as candidates for panchromatic sensitizers for TiO_2-based solar cells. Steady-state and time resolved photoluminescence spectroscopy and photocurrent measurements have been employed to identify the prevailing transfer mechanisms for photogenerated excitons between CdSe QDs capped with a traditional bulky organic ligand trioctylphosphine and Ru-dyes (N3 or Ru505) deposited onto inert glass or mesoporous TiO_2 substrates. The type II energy level alignment between the QDs and both N3 and Ru505 offers a possibility for the directional charge separation, with electrons transferred to the QDs and holes to the dye. This scenario is indeed valid for the QD/Ru505 and TiO_2/QD/Ru505 hybrid systems, with the negligible spectral overlap between the emission of the QDs and the absorption of the Ru505 dye. For the QD/N3 and TiO_2/QD/N3 hybrid systems, the spectral overlap favors the longer range energy transfer from the QDs to N3, independently of the presence of the electron acceptor TiO_2. © *2011 American Institute of Physics*. [doi:10.1063/1.3605486]

INTRODUCTION

Semiconductor nanocrystals, often referred to as colloidal quantum dots (QDs) possess a number of fascinating properties at the nanoscale.[1] In particular, the bandgap tunability by size control offers an easy way to tailor the optical absorption and emission properties of QDs, rendering them particular attractive for a wide range of applications ranging from bioimaging[2–4] to photovoltaics.[5–7] Focusing on photovoltaic applications, further attractive properties of the semiconductor QDs include hot carrier collection[8] and multiple carrier generation,[9] although their full exploitation in solar cells is not straightforward and requires further investigation. The QDs have been tested in several solar cell configurations, ranging from all-inorganic layered structures of CdSe and CdTe QDs[5,10] to the bulk-heterojunction solar cells based on semiconductor nanocrystals and conjugated polymers.[11–13] Studies of quantum dot sensitized solar cells (QDSSCs),[14] nanostructures based on a concept similar to the well-known dye sensitized solar cells (DSSCs)[15] but utilizing QDs instead of Ru-dyes as photosensitizers of mesoporous TiO_2 are receiving increasing attention at present.[16–20] Despite the potential benefits of QDs with respect to Ru-dyes, the reported maximum conversion efficiencies of QDSSCs (3–4%)[19,20] are still far behind those for DSSC (12.1%).[21] When colloidal QDs molecularly linked to mesoporous TiO_2 films are used as photosensitizers, the main limitation for the efficient QDSSC operation is often related to the low optical absorption due to the poor surface coverage of the QDs,[22] despite high internal quantum efficiencies reaching 90%.[23] On the contrary, when *in situ* grown QDs (by chemical bath deposition,[19] or sequential ionic layer adsorption and reaction)[24,25] are employed, the main loss mechanism is related to the fast internal recombination and, in this case, the internal quantum efficiencies are significantly lower (around 50%).[23] Further important limiting factors in QDSSCs are related to excessive series resistance caused by charge transfer limitations at the counterelectrode/electrolyte interface,[26] and charge recombination through surface states.[27]

In order to overcome these drawbacks and improve the efficiencies of QDSSCs, different strategies have been proposed. The introduction of nanometric barriers at the TiO_2/QD/electrolyte interface has been proven to efficiently eliminate surface recombination losses, significantly (up to two times) improving photocurrents and hence, energy conversion efficiencies.[18,19] The use of an additional encapsulating TiO_2 amorphous coating on CdSe QD sensitized TiO_2 mesoporous substrates resulted in the substitution of polysulfide redox electrolyte, for which the conventional platinum

[a)]Authors to whom correspondence should be addressed. Electronic addresses: sjulia@fca.uji.es and andrey.rogach@cityu.edu.hk.

counterelectrodes exhibit poor electrocatalytic properties,[28,29] by the standard I^-/I_3^- redox electrolyte commonly employed for DSSCs, which led to increased efficiencies while maintaining the stability of the QDs.[30] Tailoring the band alignment of the TiO_2 and CdSe QDs by the use of molecular dipoles has been shown to improve the performance of QDSSCs,[31] while the synergistic combination of nanometric barriers (ZnS conformal coating), together with the proper band alignment through the use of molecule dipoles has led to a factor of 6 enhancement in the conversion efficiency.[32]

Yet another promising strategy to improve the performance of QDSSCs is the simultaneous use of colloidal QDs and Ru-dyes as supracollectors of light in hybrid (QDs and dye) sensitized solar cells (HSSC).[33] Hybrid structures of QDs and dyes can, in an ideal case, simultaneously satisfy several important requirements for light harvesting materials: (i) extend the spectral absorption range by adding up the absorption ranges of both components,[34] (ii) reduce the internal charge recombination by fast hole scavenging from QDs and efficient spatial separation of electrons and holes via a multistep charge separation cascade,[35,36] and (iii) improve charge extraction by the reduction of recombination losses in QDs.[37] Our recent surface photovoltage study demonstrated a remarkable 40-fold enhancement in electron injection from QDs into TiO_2 for the combination of CdSe QDs and N3 dye.[33] Type II alignment of energy levels between the CdSe QDs and several types of Ru-dyes used in that study promoted electron injection from dyes into TiO_2, facilitated by the efficient extraction of holes from the valence band of QDs to the ground state of the dye. In contrast, when CdTe QDs were combined with the same Ru-dyes instead of CdSe QDs, the type I alignment resulted in nonradiative energy transfer between the QDs and the dye.[33] Both CdSe and CdTe QDs employed in that study were synthesized in water[38,39] and thus capped as-prepared with a short-chain surface ligand, thioglycolic acid (TGA, chain length ~4 Å), which does not hinder charge separation.[10]

There have been several reports on the study of the interactions between semiconductor QDs and different kinds of dyes (Ru-polypyridine complexes, Cy5, TX Red Cadavarine, Rhodamine B) resulting either in charge transfer[40–42] or in energy transfer.[43,44] These examples illustrate that the electronic coupling between the QDs and dye may be significantly different depending on the kind of dye.

The energy transfer competing with charge transfer should not necessarily be considered as detrimental for the performance of HSSCs: it can be explored in a configuration where QDs are used as antennas, nonradiatively funneling[45] absorbed light to the charge separating dye molecules.[46] Consequently, in order to better exploit the potential benefits of HSSCs, a deeper understanding of the interaction mechanisms between QDs and Ru-dyes in terms of the competition between energy transfer and charge separation is necessary. The present study employs steady-state and time-resolved photoluminescence (PL) spectroscopy along with photocurrent measurements to analyze the interactions between colloidal CdSe QDs and two Ru-dyes (N3 or Ru505), sequentially adsorbed on inert glass or mesoporous TiO_2 substrates.

EXPERIMENTAL SECTION

In contrast to our previous study,[33] the CdSe QDs (4.5 nm in diameter[47]) employed here were synthesized in organics[48] and had bulkier ligand trioctylphosphine (TOP, chain length ~11 Å) on their surface. They were carefully purified from the excess of stabilizer by three cycles of precipitation and isolation by centrifugation and redispersion, resulting in a 5×10^{-5} M stock solution in toluene. Incomplete washing of the QDs would result in an excess of organic ligands at the surface of the QDs, which would dramatically reduce the observed photocurrents.[49] Two Ru-dyes, N3 and Ru505, were purchased from Solaronix SA, Switzerland. They have a very similar chemical structure of $Ru(dcbpy)_2(X)_2$ ($dcbpy = 2,2'$-bipyridyl-4,4′-dicarboxylate) with the only difference for X being the thiocyanate group in N3 and the cyanide group in Ru505 [Fig. 1(a)].

Hybrid structures of CdSe QDs and Ru-dyes were prepared on inert glass and on the mesoporous TiO_2 substrates, to account for the possible difference in the QD-dye interactions with and without the presence of the electron acceptor, TiO_2. For the sets of samples on glass substrates, 10 μl of the stock solution of CdSe QDs in toluene were mixed with 10 μl of 5×10^{-4} M stock solution of N3 or Ru505 dye in ethanol and drop-casted onto thoroughly cleaned microscopy slides. Reference samples of bare dyes were prepared in a comparable way, mixing 10 μl of the QD stock solution with 10 μl of ethanol or 10 μl of the dye stock solution with 10 μl of toluene, followed by drop casting.

Another set of samples was prepared by the sequential adsorption of QDs and a dye on mesoporous TiO_2 substrates [Fig. 1(b)]. The latter were prepared from a colloidal titania paste containing TiO_2 nanoparticles of 20–450 nm size (Dyesol 18NR-AO) deposited on transparent SnO_2:F (FTO) coated glass electrodes (Pilkington TEC15, 15 Ω/sq resistance) and sintered at 450 °C for 30 min, resulting in ~10 μm thick films. The TiO_2 surface was functionalized with cysteine[26] to ensure the efficient adsorption of QDs. The CdSe QDs have been deposited from their stock solution in toluene by dipping TiO_2 substrates for 24 h, resulting in a homogeneous coating. The preparation of hybrid TiO_2/QD/dye samples has been accomplished by dipping TiO_2/QD substrates into a 5×10^{-5} M solution of N3 or Ru505 dye in ethanol for 2 h. The samples were rinsed with toluene after dipping in QD solution, or with ethanol after dipping in dye solution. These samples contained a relatively low amount of dye on top of the QDs, and are denoted as *low dye load* samples (L_{N3} and L_{Ru505}) in the following discussion. The preparation of reference samples of dyes was not as straightforward in this case, since TiO_2 is known to be a very strong PL quencher for Ru dyes.[50,51] Instead, we have used the following approach in order to compare the PL decays of the dyes influenced and not (or only minimally) influenced by interactions with CdSe QDs. After the measurements on the hybrid TiO_2/QD/dye samples prepared as described the same specimens were dipped into a 5×10^{-4} M ethanol solution of the respective

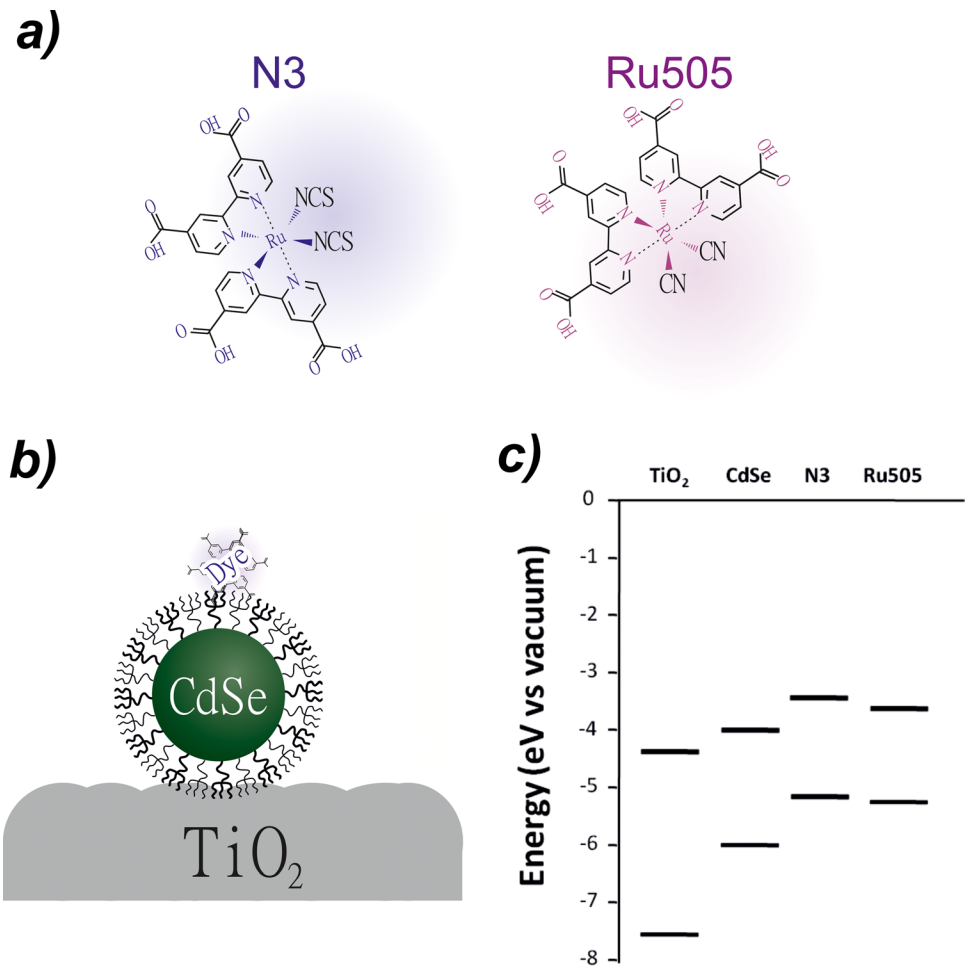

FIG. 1. (Color online) (a) Chemical structures of N3 and Ru505 dyes. (b) Scheme of a hybrid structure of CdSe QDs and a Ru-dye sequentially deposited on a TiO_2 substrate. (c) Energy diagram for TiO_2, CdSe QDs, and N3 and Ru505 dyes used in this study (see Ref. 62).

dye for 15 h in order to overload it with dye. These dye-*overloaded* structures (denoted as O_{N3} or O_{Ru505} in the following discussion) served as qualitative reference samples, since they contained a significant amount of dye molecules without a direct contact to QDs or TiO_2.

The absorption and steady-state PL spectra were taken with a Varian Cary 5000 spectrophotometer and a Horiba Jobin-Yvon Fluorolog-3 spectrometer, respectively. The excitation wavelength was 400 nm for all measurements. Time-resolved PL measurements were made with a streak camera (Hamamatsu C5680) combined with the spectrometer (Cromex, 40 gr/mm grating). The frequency doubled output of the mode-locked titanium-sapphire laser (150 fs, 100 kHz) was used as an excitation source at 400 nm. The emission wavelength range selected for monitoring the PL decays (Table I) was determined by the fitting of the steady state PL spectra to a Gaussian function and extracting the peak maximum (λ_{max}) and the FWHM standard deviation (σ). The emission range was ($\lambda_{max} \pm \sigma$).

Photocurrent measurements have been done in a three-electrode configuration using the sensitized TiO_2 electrodes as the working electrode, a Pt wire as the counterelectrode and a Ag/AgCl reference electrode. As an electrolyte, 0.01 M tetrabutylammonium tetrafluoroborate in methanol has been employed, with methanol acting as a hole scavenger. A Xe lamp coupled with a UV filter was used for illumination, in order to avoid the direct photoexcitation of electron-hole pairs in TiO_2. The illumination power was 20 mW/cm^2.

RESULTS AND DISCUSSION

The type II alignment of the energy levels of the CdSe QDs and both N3 and Ru505 dyes, with the lowest excited energy state for the electrons in QDs and for holes in the dye [Fig. 1(c)] makes the possibility of charge separation in their hybrid systems evident. In the case of sequentially deposited layers of TiO_2, CdSe QDs, and the dyes [Fig. 1(b)], the presence of the strong electron acceptor TiO_2 may additionally facilitate the extraction of electrons from the QDs. The charge separation is based on the wavefunction overlap

TABLE I. Emission range selected for monitoring PL decays after fitting the steady state PL spectra to a Gaussian function (peak maximum, λ_{max}, and standard deviation, σ).

System	λ_{max} (nm)	σ (nm)	Emission range (nm)
N3; QD/N3	772	45	727–817
Ru505; QD/Ru505	689	54	635–743
TiO_2/N3; TiO_2/QD/N3	712	24	688–736
TiO_2/Ru505; TiO_2/QD/Ru505	710	48	662–758

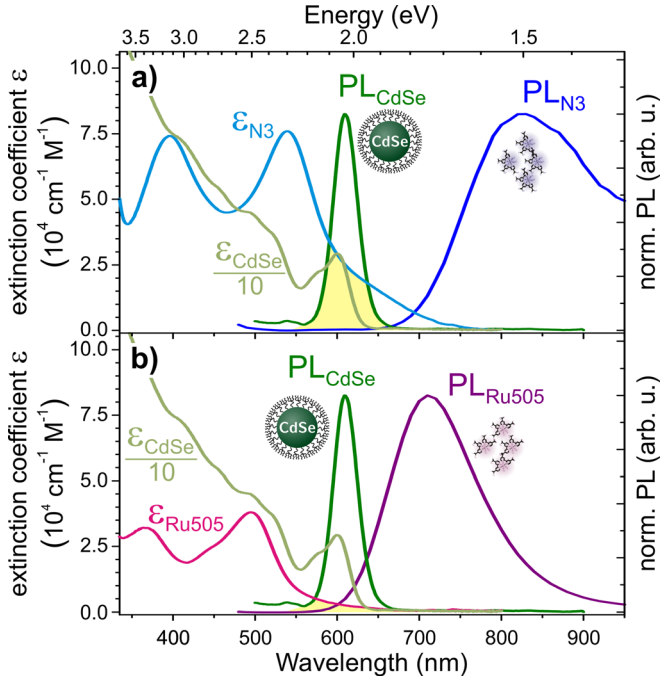

FIG. 2. (Color online) Absorption and steady state PL spectra of (a) N3 and (b) Ru505 dye. Absorption and PL spectra of CdSe QDs are presented in both graphs to indicate the spectral overlap (yellow-shadowed areas) relevant for nonradiative energy transfer.

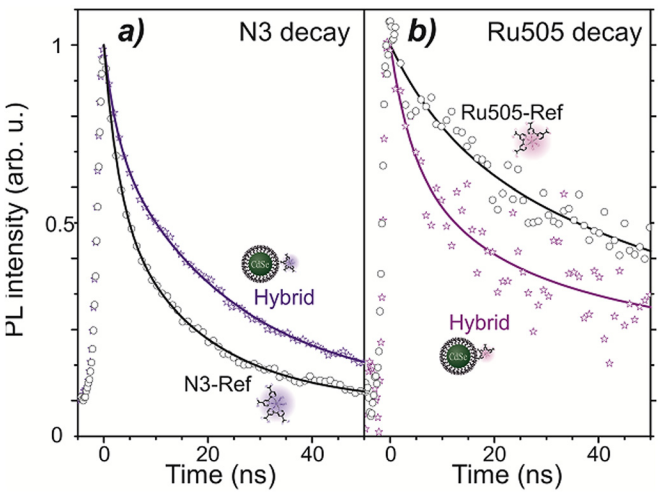

FIG. 3. (Color online) Time-resolved PL decays of (a) N3 and (b) Ru505 dyes in hybrid CdSe QDs/dye systems on inert glass substrates, compared to the respective reference samples of the N3 and Ru505 dyes only. The solid lines are the best fits to the experimental points. Selected emission ranges are specified in the experimental section (Table I).

and follows the exponential distance dependence between the two partners. On the contrary, the Förster resonance energy transfer (FRET) can take place between the two partners with different bandgaps, with the excitons transferred from a material with the higher bandgap (donor) to the material with the lower bandgap (acceptor).[52] The distance dependence of the FRET rate is influenced by the geometrical arrangement of the donor and acceptor species,[53] ranging from d^{-6} to d^{-3}. The energy transfer is independent on the band alignment and can also occur in parallel with charge separation. One important condition for the energy transfer is the spectral overlap of the emission spectrum of the donor with the absorption of the acceptor. A longer acceptor lifetime is normally characteristic for FRET and shows the "feeding" of the acceptor from the donor via energy transfer.

Figure 2 shows the absorption and PL spectra of both of the dyes and the QDs employed. Both N3 and Ru505 absorption spectra are characterized by the presence of two bands, with the peak positions at 395 and 530 nm for N3 and at 365 and 490 nm for Ru505. Their emission spectra are characterized by a broad peak located between 700 and 950 nm for N3 and between 600 and 850 nm for Ru505. The absorption and emission spectra of CdSe QDs are shown in both Figs. 2(a) and (b) to demonstrate the spectral overlap (yellow-shadowed areas) of the emission of CdSe QDs with the absorption of dye. The spectral overlap is larger for N3 than for Ru505, indicating the higher probability of energy transfer from QDs to N3. At the same time, the charge separation between the QDs and both kinds of dyes is possible due to the type II energy level alignment of the components [Fig. 1(c)]. The energy transfer should lead to the quenching of QD emission and the increase of the emission of dye, while the charge transfer should result in the quenching of emission of both components.

Due to the inhomogeneity of the samples and strong light scattering by the TiO_2 films, the discrimination between the energy transfer and the charge separation processes is not possible via steady-state PL and absorption characterization. Therefore, we have performed time-resolved PL measurements, monitoring the PL decays of dyes in the hybrid QD/dye composites. The PL decays of the dyes can be influenced by two processes: energy transfer from the QDs to the dye resulting in the feeding of the dye whose PL decay becomes slower, or a charge transfer which dissociates excitons in both QDs and the dye, causing the dye to decay faster. A comparison of the PL decays of hybrid QD/dye samples with the respective reference samples of bare dyes deposited on inert glass substrates shows that the former scenario is valid for the N3 dye [Fig. 3(a)], while the latter takes place for Ru505 [Fig. 3(b)]. This shows that, despite the type II alignment of energy levels, the energy transfer prevails over the charge transfer in the hybrid QD/N3 system, due to the large enough spectral overlap of the emission of the QDs and the absorption of the N3 [Fig. 2(a)]. The respective spectral overlap for the hybrid system, QD/Ru505, is negligible [Fig. 2(b)], and the charge separation takes over.

Since hybrid structures of QDs and Ru-dyes are particularly interesting for their application as potential co-sensitizers in TiO_2-based solar cells, we compared the PL decays for the hybrid QD/N3 and QD/Ru505 structures deposited on mesoporous TiO_2 substrates [Fig. 4]. The results obtained show the same trends as for inert glass substrates: a slower PL decay of the N3 dye in the hybrid TiO_2/QD/N3 sample, L_{N3}, as compared to the N3-overloaded specimen, O_{N3} [Fig. 4(a)], and a faster PL decay of the Ru505 dye in the hybrid TiO_2/QD/Ru505 sample, L_{Ru505}, as

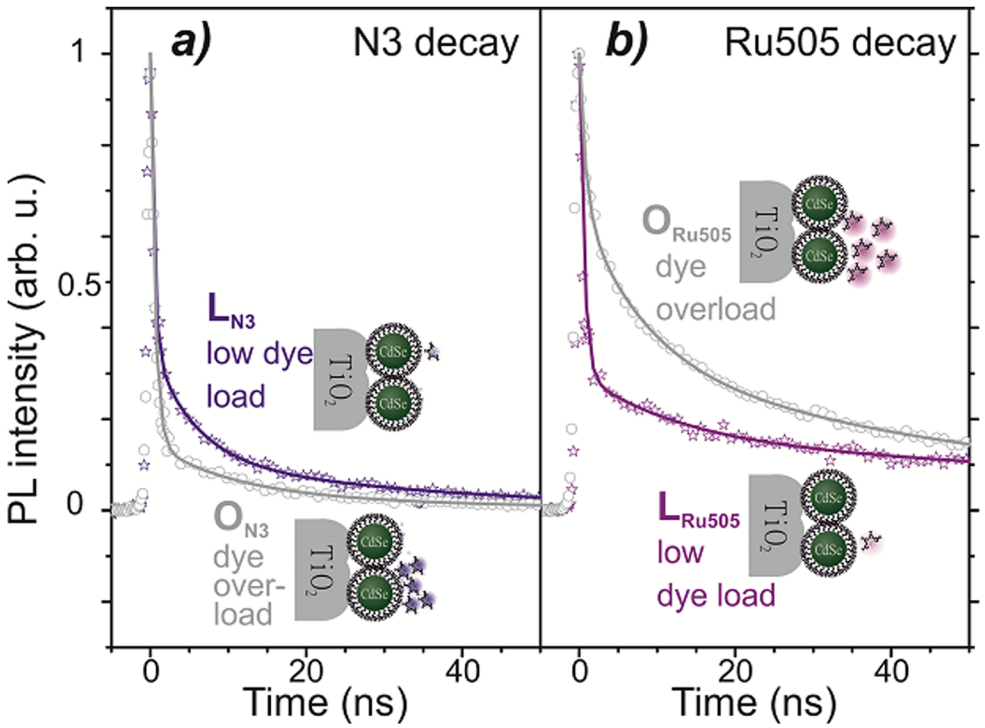

FIG. 4. (Color online) Time-resolved PL decays of (a) N3 and (b) Ru505 dyes in the hybrid CdSe QDs/dye systems with low dye load (samples L_{N3} and L_{Ru505}) on mesoporous TiO_2 substrates, compared to the reference samples overloaded with respective dyes (O_{N3} and O_{Ru505}). The solid lines are the best fits to the experimental points. The selected emission ranges are specified in the experimental section (Table I).

compared to the Ru505-overloaded specimen, O_{Ru505} [Fig. 4(b)].

The photocurrent response of the systems under study has been measured as previously detailed in Sec. II. The obtained results show that both QD/dye hybrid systems provide higher photocurrents compared to the dye-only and QDs-only samples [Fig. 5]. These results are consistent with the energy and charge transfer in the hybrid QD/N3 and QD/Ru505 systems, respectively, supporting the results of the PL measurements. In addition, both hybrid systems present a higher pseudo-open-circuit voltage potential, V_{oc} (voltage at photocurrent zero), as compared to dye-only sensitized TiO_2 electrodes (Fig. 5). We use the prefix 'pseudo' to indicate that this is not the standard V_{oc} measured in the two-electrode

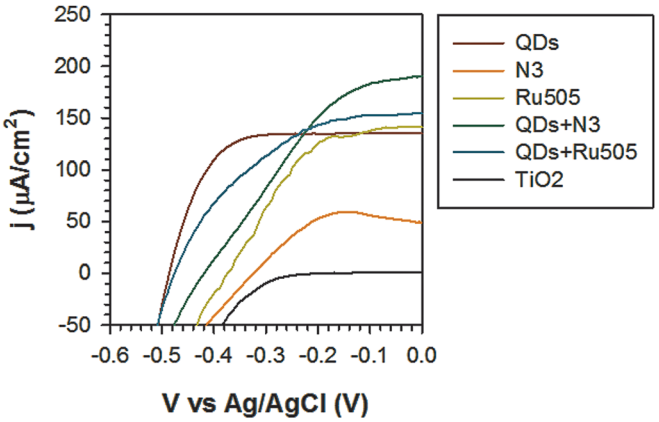

FIG. 5. (Color online) Photocurrent measurements: current density/voltage curves obtained for TiO_2 electrodes sensitized with different combinations of CdSe QDs and Ru-dyes in a three-electrode configuration. The response of the bare TiO_2 electrode is also included for comparison.

configuration: V_{oc} depends only on the photovoltaic properties of the system, while the pseudo-V_{oc}, measured with the three-electrode configuration, also depends on the type of reference electrode used. The increase of the pseudo-V_{oc} for the hybrid systems is consistent with an increase of the charge separation between the photo-injected electrons in the TiO_2 and the holes in the dye. This charge separation, promoted by both energy and charge transfer, increases for hybrid samples, reducing the recombination with a subsequent increase of pseudo-V_{oc}.

Our results show that, independent of the presence of a mesoporous TiO_2 substrate, the energy transfer takes place between the QDs and the N3 dye, while the charge transfer occurs between QDs and the Ru505 dye. According to the estimated position of the energy levels [Fig. 1(c)], a type II alignment should exist for the CdSe QDs and both dyes, with an even larger offset between the conduction band of the QDs and the LUMO of N3 (Ref. 33) compared to the LUMO of Ru505,[54] which should result in a higher driving force for the charge separation in the QD/N3 hybrid system.[55] At the same time, the spectral overlap of the emission of the QDs and the absorption of the dye favors the energy transfer between CdSe and the N3 dye.[56] The charge separation in the system under study may be considered unfavorable by the relatively large (2.5–3 nm) distance between the dye molecule and the QD core, due to the large QD diameter (4.5 nm) and bulky TOP ligands (1.1 nm) on the QD surface,[47] although there have been reports that Ru dyes may directly anchor to the surface of the CdSe QDs by their carboxylate-containing ligands.[40,57] The energy transfer relies on long range dipole-dipole interactions, with typical Förster radii in the range of 5–6 nm,[56,58] and can thus compete with the charge separation in the case of a favorable spectral overlap.

The chemical structures of both dyes studied here differ in two thiocyanate groups being present in N3 and two cyanide groups in Ru505. The presence of these functional groups, offering a different ability to coordinate with the Cd-rich surface of the CdSe QDs[59] or penetrate into the shell of the TOP molecules may additionally affect QD-dye interactions and thus the transfer mechanisms.

CONCLUSIONS

Our data, together with the results of our recent related studies[33,55] demonstrate that the competition between the charge separation and energy transfer in hybrid systems of semiconductor QDs and Ru-dyes (or polymers[55]) strongly depends on the energy level alignment and spectral overlap. Independently of the presence of the TiO_2 substrate, energy transfer takes place from the CdSe QDs capped by bulky TOP ligands to the N3 dye, while for the similar hybrid system of N3 dyes and CdSe QDs capped by short-chain TGA molecules, the charge transfer has previously been identified by the surface photovoltage spectroscopy as a prevailing mechanism.[33] Our results show that beyond energetic considerations, the interactions of the components of the hybrid systems under study determined by the surface ligands of QDs and the functional groups of the dyes may influence the transfer mechanism. The role of the capping ligands of the colloidal QDs has been demonstrated to have paramount importance on the efficient charge separation at the QD/polymer interface.[60] Consequently, it is expected that the nature of capping ligands is also crucial for governing the QD-dye interaction. The future development of these supracollector structures for photovoltaic applications will rely on tailoring the interactions between the constituting entities, not only by energy level alignment but also by the anchoring groups of the dye molecules, the capping molecules of the QDs, and the supracollector geometries for maximizing their light harvesting capabilities, optimizing the transfer mechanism for optimum electron injection into wide bandgap semiconductors (TiO_2, ZnO), and hole scavenging dynamics. There have already been recent reports demonstrating the beneficial effect of the co-sensitization of QDs and dyes in full device architectures. As an example, Liu and Wang have demonstrated the enhanced performance of the hybrid PbS QD/N719 dye structure (6.35% efficiency), compared to only N719 (5.95% efficiency).[61]

ACKNOWLEDGMENTS

This work was supported by the Ministerio de Educación y Ciencia of Spain under the projects HOPE CSD2007-00007 (Consolider-Ingenio 2010), JES-NANOSOLAR PLE2009-0042 and MAT2007-62982, by Generalitat Valenciana project PROMETEO/2009/058, by the GRF project 102810 from the Research Grants Council of Hong Kong, and by the European FP7 program through ITN "ICARUS" (237900). SG acknowledges the financial support of the Spanish Ministerio de Ciencia e Innovación through the Ramón y Cajal program and the Generalitat Valenciana for the grant BEST/2009/147.

[1] *Semiconductor Nanocrystal Quantum Dots: Synthesis, Assembly, Spectroscopy and Applications*, edited by A. L. Rogach (Springer, Wien-New York, 2008).
[2] X. Michalet, F. F. Pinaud, L. A. Bentolila, J. M. Tsay, S. Doose, J. J. Li, G. Sundaresan, A. M. Wu, S. S. Gambhir, and S. Weiss, Science **307**, 538 (2005).
[3] I. L. Medintz, H. T. Uyeda, E. R. Goldman, and H. Mattoussi, Nature Mater. **4**, 435 (2005).
[4] A. L. Rogach, and M. Ogris, Curr. Opin. Mol. Ther. **12**, 331 (2010).
[5] I. Gur, N. A. Fromer, M. L. Geier, and A. P. Alivisatos, Science **310**, 462 (2005).
[6] P. V. Kamat, J. Phys. Chem. C **112**, 18737 (2008).
[7] E. Holder, N. Tessler, and A. L. Rogach, J. Mater. Chem. **18**, 1064 (2008).
[8] A. J. Nozik, Physica E (Amsterdam) **14**, 115 (2002).
[9] R. D. Schaller, M. Sykora, J. M. Pietryga, and V. I. Klimov, Nano Lett. **6**, 424 (2006).
[10] D. Gross, I. Mora-Sero, T. Dittrich, A. Belaidi, C. Mauser, A. J. Houtepen, E. Da Como, A. L. Rogach, and J. Feldmann, J. Am. Chem. Soc. **132**, 5981 (2010).
[11] W. U. Huynh, J. J. Dittmer, and A. P. Alivisatos, Science **295**, 2425 (2002).
[12] M. Pientka, V. Dyakonov, D. Meissner, A. L. Rogach, D. V. Talapin, H. Weller, L. Lutsen, and D. Vanderzande, Nanotechnology **15**, 163 (2004).
[13] S. Dayal, N. Kopidakis, D. C. Olson, D. S. Ginley, and G. Rumbles, Nano Lett. **10**, 239 (2010).
[14] S. Rühle, M. Shalom, and A. Zaban, Chem. Phys. Chem. **11**, 2290 (2010).
[15] B. Oregan and M. Grätzel, Nature **353**, 737 (1991).
[16] I. Robel, V. Subramanian, M. Kuno, and P. V. Kamat, J. Am. Chem. Soc. **128**, 2385 (2006).
[17] H. J. Lee, H. C. Leventis, S. Moon, P. Chen, S. Ito, S. A. Haque, T. Torres, F. Nüesch, T. Geiger, S. M. Zakeeruddin, M. Grätzel, and M. K. Nazeeruddin, Adv. Funct. Mater. **19**, 2735 (2009).
[18] S. Giménez, I. Mora-Seró, L. Macor, N. Guijarro, T. Lana-Villarreal, R. Gómez, L. J. Diguna, Q. Shen, T. Toyoda, and J. Bisquert, Nanotechnology **20**, 295204 (2009).
[19] L. J. Diguna, Q. Shen, J. Kobayashi, and T. Toyoda, Appl. Phys. Lett. **91**, 0231161 (2007).
[20] S. Q. Fan, B. Fang, J. H. Kim, J. J. Kim, J. S. Yu, and J. Ko, Appl. Phys. Lett. **96**, 063501 (2010).
[21] Q. Yu, Y. Wang, Z. Yi, N. Zu, J. Zhang, M. Zhang, and P. Wang, ACS Nano **4**, 6032 (2010).
[22] N. Guijarro, T. Lana-Villarreal, I. Mora-Seró, J. Bisquert, and R. Gómez, J. Phys. Chem. C **113**, 4208 (2009).
[23] S. Giménez, T. Lana-Villarreal, R. Gómez, S. Agouram, V. Muñoz-Sanjosé, and I. Mora-Seró, J. Appl. Phys. **108**, 064310 (2010).
[24] H. J. Lee, M. Wang, P. Chen, D. R. Gamelin, S. M. Zakeeruddin, M. Grätzel, and M. K. Nazeeruddin, Nano Lett. **9**, 4221 (2009).
[25] V. González-Pedro, X. Xu, I. Mora-Seró, and J. Bisquert, ACS Nano **4**, 5783 (2010).
[26] I. Mora-Seró, S. Giménez, T. Moehl, F. Fabregat-Santiago, T. Lana-Villareal, R. Gómez, and J. Bisquert, Nanotechnology **19**, 4240071 (2008).
[27] I. Mora Seró, S. Giménez, F. Fabregat Santiago, R. Gómez, Q. Shen, T. Toyoda, and J. Bisquert, Acc. Chem. Res. **42**, 1848 (2009).
[28] G. Hodes, J. Manassen, and D. Cahen, J. Electrochem. Soc. **127**, 544 (1980).
[29] S. Licht, O. Khaselev, P. A. Ramakrishnan, T. Soga, and M. Umeno, J. Phys. Chem. B **102**, 2536 (1998).
[30] M. Shalom, S. Dor, S. Rühle, L. Grinis, and A. Zaban, J. Phys. Chemi. C **113**, 3895 (2009).
[31] M. Shalom, S. Ruhle, I. Hod, S. Yahav, and A. Zaban, J. Am. Chem. Soc, **131**, 9876 (2009).
[32] E. Barea, M. Shalom, S. Giménez, I. Hod, I. Mora-Seró, A. Zaban, and J. Bisquert, J. Am. Chem. Soc. **132**, 6834 (2010).
[33] I. Mora-Sero, D. Gross, T. Mittereder, A. A. Lutich, A. S. Susha, T. Dittrich, A. Belaidi, R. Caballero, F. Langa, J. Bisquert, and A. L. Rogach, Small **6**, 221 (2010).
[34] M. Shalom, J. Albero, Z. Tachan, E. Martinez-Ferrero, A. Zaban, and E. Palomares, J. Phys. Chem. Lett. **1**, 1134 (2010).
[35] I. Mora-Seró, T. Dittrich, A. S. Susha, A. L. Rogach, and J. Bisquert, Thin Solid Films **516**, 6994 (2008).
[36] I. Mora-Seró, V. Likodimos, S. Giménez, E. Martínez-Ferrero, J. Albero, E. Palomares, A. G. Kontos, P. Falaras, and J. Bisquert, J. Phys. Chem. C **114**, 6755 (2010).
[37] H. C. Leventis and S. A. Haque, Energy Environ. Sci. **2**, 1176 (2009).

[38]A. L. Rogach, A. Kornowski, M. Gao, A. Eychmüller, and H. Weller, J. Phys. Chem. B **103**, 3065 (1999).
[39]N. Gaponik and A. L. Rogach, Phys. Chem. Chem. Phys. **12**, 8685 (2010).
[40]M. Sykora, M. A. Petruska, J. Alstrum-Acevedo, I. Bezel, T. J. Meyer, and V. I. Klimov, J. Am. Chem. Soc. **128**, 9984 (2006).
[41]J. Huang, D. Stockwell, Z. Huang, D. L. Mohler, and T. Lian, J. Am. Chem. Soc. **130**, 5632 (2008).
[42]S. N. Sharma, Z. S. Pillai, and P. V. Kamat, J. Phys. Chem. B **107**, 10088 (2003).
[43]K. Becker, J. M. Lupton, J. Müller, A. L. Rogach, D. V. Tapalin, H. Weller, and J. Feldmann, Nature Mater. **5**, 777 (2006).
[44]A. M. Funston, J. J. Jasieniak, and P. Mulvaney, Adv. Mater. **20**, 4274 (2008).
[45]T. Franzl, T. A. Klar, S. Schietinger, A. L. Rogach, and J. Feldmann, Nano Lett. **4**, 1599 (2004).
[46]S. Buhbut, S. Itzhakov, E. Tauber, M. Shalom, I. Hod, G. Geiger, Y. Garini, D. Oron, and A. Zaban, ACS Nano **4**, 1293 (2010).
[47]W. W. Yu, L. Qu, W. Guo, and X. Peng, Chem. Mater. **15**, 2854 (2003).
[48]Q. Wang, D. Pan, S. Jiang, X. Ji, L. An, and B. Jiang, J. Cryst. Growth **286**, 83 (2006).
[49]A. Biebersdorf, R. Dietmüller, A. S. Susha, A. L. Rogach, S. K. Poznyak, D. V. Talapin, H. Weller, T. A. Klar, and J. Feldmann. Nano Lett. **6**, 1559 (2006).
[50]G. Benko, P. Myllyperkio, J. Pan, A. P. Yartsev, and V. Sundstrom, J. Am. Chem. Soc. **125**, 1118 (2003).
[51]J. B. Asbury, N. A. Anderson, E. C. Hao, X. Ai, and T. Q. Lian, J. Phys. Chem. B **107**, 7376 (2003).
[52]T. Förster, Ann. Phys. **2**, 55 (1948).
[53]A. L. Rogach, T. A. Klar, J. M. Lupton, A. Meijerink, and J. Feldmann, J. Mater. Chem. **19**, 1208 (2009).
[54]G. Sauvé, M. E. Cass, S. J. Doig, I. Lauermann, K. Pomykal, and N. S. Lewis, J. Phys. Chem. B **104**, 3488 (2000).
[55]A. A. Lutich, G. Jiang, A. S. Susha, A. L. Rogach, F. D. Stefani, and J. Feldmann, Nano Lett. **9**, 2636 (2009).
[56]M. A. Petruska, A. P. Bartko, and V. I. Klimov, J. Am. Chem.Soc. **126**, 714 (2004).
[57]M. Sykora, M. A. Petruska, J. Alstrum-Acevedo, I. Bezel, T. J. Meyer, and V. I. Klimov, J. Am. Chem. Soc. **128**, 9984 (2006).
[58]I. L. Medintz, A. R. Clapp, H. Mattoussi, E. R. Goldman, B. Fisher, and J. M. Mauro, Nature Mater. **2**, 630 (2003).
[59]M. Du, C. P. Li, and J. H. Guo, Inorg. Chim. Acta **359**, 2575 (2006).
[60]E. Martinez-Ferrero, J. Albero, and E. Palomares, J. Phys. Chem. Lett. **1**, 3039 (2010).
[61]Y. Liu and J. Wang, Thin Solid Films **518**, e54 (2010).
[62]See supplementary material at http://dx.doi.org/10.1063/1.3605486 for an energy diagram showing type I and type II alignment in the hybrid systems under study; a schematic illustration showing the binding of QDs to TiO2 surface by cysteine molecules; and details on the estimation of energy level positions for TiO2, QDs, and dyes.